J. Fluid Mech. (1977), *vol.* 79, *part* 4, *pp.* 689–702
Printed in Great Britain

Weakly nonlinear stability of a viscous free shear layer

By S. A. MASLOWE

Department of Mathematics, McGill University,
Montreal, Quebec, Canada

(Received 15 September 1975)

Numerical calculations of the Landau constant are presented for the case of a shear layer of finite Reynolds number, having the velocity profile $\bar{u} = \tanh y$. It is found that this parameter has a strong dependence on the Reynolds number for $Re \leqslant 100$. In particular, the Landau constant is reduced by 43 % from its inviscid value when $Re = 40$, the latter value being typical of many experiments. This percentage, however, is based upon a calculation in which the mean-flow distortion has been neglected. A rough estimate of the latter effect indicates that it could possibly increase the value of the Landau constant sufficiently that the net influence of a finite Reynolds number would be of a smaller magnitude.

1. Introduction

The weakly nonlinear stability theory for shear flows was formulated in 1960 by Stuart and Watson, who showed that the temporal evolution of the perturbation amplitude A_1 was governed by an equation of the form

$$A_1^{-1} dA_1/dt = a_0 + a_2|A_1|^2 + O(|A_1|^4). \tag{1.1}$$

If one is in a frame of reference moving with the wave speed, then the quantity a_0 can be identified with αc_i, the amplification factor of linearized theory; however, it is a_2, the 'Landau constant', that is of central interest in the nonlinear theory. The first quantitative calculation of a_2 was made by Schade (1964) for the $\tanh y$ mixing-layer profile at a finite but very large Reynolds number. Schade obtained the result $a_2 = -16/3\pi$, thus establishing the existence of a supercritical equilibrium state for modes sufficiently close to the neutral wavenumber $\alpha_n = 1$.

Subsequently, Stuart (1967) computed inviscid equilibrium states to higher order by expanding the wavenumber about its neutral value. The methods used by Schade and Stuart at first glance seem to be equivalent; however, in the time-dependent approach it is necessary to use viscosity to treat singularities that arise, whereas this difficulty is not encountered if one computes only steady states as was done by Stuart. Some subtle differences occur in the equilibrium solutions as a result; for example, the vorticity distributions are not the same, as discussed in § 4 of Stuart's paper.

More recently, the time-dependent problem was considered on an inviscid basis by Benney & Maslowe (1975), who dealt with the singularity by employing the nonlinear critical-layer concept. They obtained, instead of (1.1), a second-order amplitude equation which also included spatial variations. By using a normal-mode approach and considering the behaviour of the resulting ordinary differential equation in the phase plane, one can conclude that the steady solutions, which correspond to those determined by Stuart, are stable centres. Of these three investigations, the present work is most closely related to that of Schade as its purpose is to investigate finite Reynolds number effects in a weakly nonlinear context.

A number of experiments have been reported for flows that are well approximated by the $\tanh y$ profile (see, for example, Miksad (1972) and references cited therein). Of course, one would like to compare the experimental results with those of the finite amplitude theory; however, such a comparison can provide only a qualitative indication of the accord between the two, because the theory is valid only for wavenumbers sufficiently close to the neutral curve. In fact, Stuart (1967) estimated that his expansion converges only for $0{\cdot}975 \leqslant \alpha \leqslant 1{\cdot}0$,† whereas α_M, the fastest-growing wave of linearized theory, is equal to 0·445, as first computed by Michalke (1964). None the less, if one wishes to make such comparisons (as several authors have done), the conditions for doing so are more favourable at finite Re because both $|\alpha_n - \alpha_M|$ and αc_i decrease with decreasing Re (see figure 1). Here α_n denotes the neutral wavenumber. Further discussion of these matters is postponed until § 5 in order that the results for a_2 as a function of Re can first be presented.

2. General theory

To begin with, we outline the basic approach with the aid of figure 1, which shows the linear neutral-stability curve for the $\tanh y$ profile. Let us focus attention upon a linearly unstable mode having, for example, the values of α and Re that correspond to point B. The temporal evolution and subsequent equilibration of this mode are to be computed by perturbing away from the point A on the linear neutral curve that has the *same* Reynolds number as B. Note that a perturbation about some critical Re is not appropriate for this problem because the instability mechanism is inviscid.

Proceeding now to the analysis, our starting point is the non-dimensional vorticity equation, which can be written as

$$\nabla^2\psi_t + \psi_y \nabla^2\psi_x - \psi_x \nabla^2\psi_y = Re^{-1}\nabla^2(\nabla^2\psi), \tag{2.1}$$

where $Re = U_0 L/\nu$, ν being the kinematic viscosity. We consider a parallel shear flow with velocity profile $\bar{u}(y)$ and superimpose upon the basic flow a small perturbation that propagates with phase speed c. The method of multiple time scales will be employed, so that the time derivative in (2.1) is transformed according to

$$\frac{\partial}{\partial t} \to \frac{\partial}{\partial t} + \alpha\epsilon^2 \frac{\partial}{\partial \tau},$$

† Note, however, that the convergence of this series can be somewhat improved by using Shank's (1955) transformation.

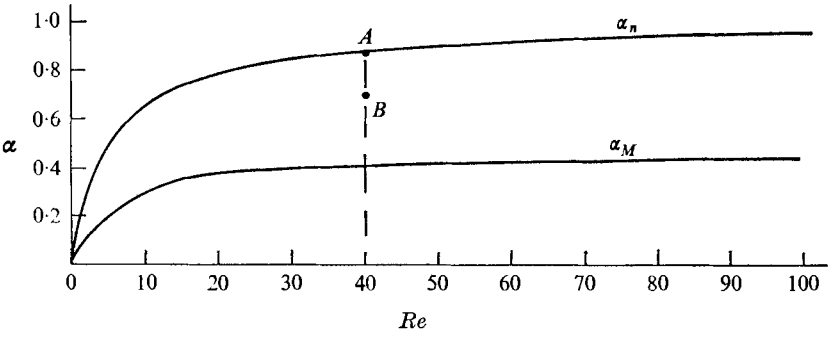

FIGURE 1. Stability boundary and wavenumber of fastest-growing wave according to linear theory.

where ϵ is an amplitude parameter that can be set equal to $c_i^{\frac{1}{2}}$ (i.e. even though the quantity c_i does not exist in the nonlinear theory, it is useful to refer to the value of c_i that linear theory would predict at a point such as B in figure 1), and the amplitude of the wave evolves on the slow time scale $\tau = \alpha\epsilon^2 t$.

It is convenient to employ a co-ordinate system moving with the wave speed, so that $\partial/\partial t = 0$ and we write

$$\psi = \int_{y_c}^{y} \{\bar{u}(y) - c\}\, dy + \epsilon\hat{\psi}(\theta, y, \tau), \tag{2.2}$$

where $\theta = \alpha x$. The perturbation stream function $\hat{\psi}$ is found to satisfy the equation

$$\epsilon^2\nabla^2\hat{\psi}_\tau + (\bar{u}-c)\,\nabla^2\hat{\psi}_\theta - \bar{u}''\hat{\psi}_\theta + \epsilon(\hat{\psi}_y\,\nabla^2\hat{\psi}_\theta - \hat{\psi}_\theta\,\nabla^2\hat{\psi}_y) = (\alpha Re)^{-1}\nabla^2(\nabla^2\hat{\psi}), \tag{2.3}$$

where $\nabla^2 = \alpha^2\partial^2/\partial\theta^2 + \partial^2/\partial y^2$. The solution of (2.3) is to be found by expanding $\hat{\psi}$ as follows:

$$\begin{aligned}\epsilon\hat{\psi} \sim{}& \epsilon\{\phi_1(\tau, y)\, e^{i\theta} + \phi_1^*\, e^{-i\theta}\} + \epsilon^2\{\phi_2(\tau, y)\, e^{2i\theta} + *\} \\ &+ \epsilon^3\{\phi_{31}(\tau, y)\, e^{i\theta} + * + \phi_{33}(\tau, y)\, e^{3i\theta} + *\} + O(\epsilon^4).\end{aligned} \tag{2.4}$$

In addition, α is expanded about its neutral value in a series having the form

$$\alpha \sim \alpha_n + \epsilon^2\alpha_2 + \ldots. \tag{2.5}$$

A few words apropos of the expansion (2.5) would seem to be in order; the form of (2.5) can be deduced in advance by recognizing that viscosity simply exerts a slight damping effect on the inviscid instability of inflexion-point profiles. From Lin's perturbation formula applied to the case $\bar{u} = \tanh y$ (see, for example, Stuart 1967, p. 425) one obtains

$$\alpha c_i \simeq (2/\pi)(1-\alpha), \tag{2.6}$$

where $\alpha_n = 1$ in the inviscid limit, so we expect that $\alpha c_i \sim \alpha_n - \alpha$ in general. Since αc_i is $O(\epsilon^2)$ in the present formulation, the expansion (2.5) follows.

We now substitute (2.4) and (2.5) into (2.3) and separate out equal powers of ϵ. In the $O(\epsilon)$ problem, the variables are separated by setting

$$\phi_1(\tau, y) = A(\tau)\,\Phi_1(y),$$

which leads to the Orr–Sommerfeld problem of linearized theory, viz.

$$\mathscr{L}\Phi_1 \equiv (\bar{u}-c)(\Phi_1''-\alpha_n^2\Phi_1)-\bar{u}''\Phi_1+(i/\alpha_n Re)(\Phi_1^{iv}-2\alpha_n^2\Phi_1''+\alpha_n^4\Phi_1)=0, \quad (2.7)$$

with the boundary conditions that Φ_1 and its derivatives vanish as $y\to\pm\infty$. It is possible, however, to exploit the symmetry of the $\tanh y$ profile and thereby reduce the range of integration to the semi-infinite domain $-\infty\leqslant y\leqslant 0$. This is further discussed in § 3, which deals with the numerical methods employed.

At $O(\epsilon^2)$, we write $\phi_2 = A^2\Phi_2(y)$ and find that Φ_2 satisfies

$$(\bar{u}-c)(\Phi_2''-4\alpha_n^2\Phi_2)-\bar{u}''\Phi_2+(i/2\alpha_n Re)(\Phi_2^{iv}-8\alpha_n^2\Phi_2''+16\alpha_n^4\Phi_2) = \tfrac{1}{2}(\Phi_1\Phi_1'''-\Phi_1'\Phi_1''), \quad (2.8)$$

with homogeneous boundary conditions whose explicit form is given in § 3. There is also a mean-flow distortion at $O(\epsilon^2)$; however, this effect, which is less significant for free shear layers than for bounded flows, will be neglected for the moment because its proper computation would require that the basic flow itself be a solution of the Navier–Stokes equations, e.g. a non-parallel flow. This matter is discussed at greater length in § 5 and a procedure for estimating the distortion effect is described in the appendix.

It is at $O(\epsilon^3)$ that the slow time dependence first enters the analysis and the amplitude equation will be seen to emerge as a result. Writing $\phi_{31} = A^2A^*\Phi_{31}(y)$ and considering all terms multiplied by $e^{i\theta}$ leads to the equation

$$A^2A^*\mathscr{L}\Phi_{31} = i\frac{dA}{d\tau}(\Phi_1''-\alpha_n^2\Phi_1)+2\alpha_2\alpha_n(\bar{u}-c)\Phi_1 A - A^2A^*G(y)+O\left(\frac{\alpha_2}{Re}\right), \quad (2.9)$$

where

$$G(y) \equiv 2\Phi_1'^*(\Phi_2''-3\alpha_n^2\Phi_2)+\Phi_1^*(\Phi_2'''-3\alpha_n^2\Phi_2')-(2\Phi_2\Phi_1'''^*+\Phi_2'\Phi_1''^*).$$

A necessary and sufficient condition for the existence of a solution to (2.9) is that the right-hand side be orthogonal to the solution of the adjoint problem. The latter consists of solving the equation

$$(\bar{u}-c)(\chi''-\alpha_n^2\chi)+2\bar{u}'\chi'+(i/\alpha_n Re)(\chi^{iv}-2\alpha_n^2\chi''+\alpha_n^4\chi)=0 \quad (2.10)$$

subject to appropriate homogeneous boundary conditions that are stated in § 3. Imposing the orthogonality condition leads to the following result:

$$i\frac{dA}{d\tau}\int_{-\infty}^{\infty}\chi(\Phi_1''-\alpha_n^2\Phi_1)\,dy+2\alpha_2\alpha_n A\int_{-\infty}^{\infty}\chi(\bar{u}-c)\Phi_1\,dy-A^2A^*\int_{-\infty}^{\infty}\chi G\,dy=0. \quad (2.11)$$

Equation (2.11) is clearly equivalent to the Landau equation (1.1). Thus the numerical solution of (2.7)–(2.11) leads to the determination of the coefficients appearing in that equation.

3. Numerical procedures

The eigenvalue problem associated with the Orr–Sommerfeld equation (2.7) has been solved using a procedure very similar to that employed by Betchov & Szewczyk (1963), who computed curves of constant αc_i for $0\leqslant Re\leqslant 40$. A fourth-order Runge–Kutta subroutine was used to integrate (2.7) and double-

precision complex arithmetic was employed throughout the computations. By taking advantage of the symmetry noted earlier it was possible to obtain satisfactory results for Re as large as 200.

The numerical integration was initiated at $y = -3$ using the asymptotic behaviour

$$\Phi_1 = A_1 e^{\alpha y} + A_3 \exp\{\alpha(1+iRe/\alpha)^{\frac{1}{2}} y\} \quad \text{as} \quad y \to -\infty, \tag{3.1}$$

which is obtained by setting $\bar{u} = -1$ and $\bar{u}'' = 0$ in (2.7). By taking the real part of Φ_1 to be even and the imaginary part to be odd, the boundary conditions at $y = 0$ become

$$\Phi_{1r}'(0) = \Phi_{1r}'''(0) = \Phi_{1i}(0) = \Phi_{1i}''(0) = 0. \tag{3.2}$$

Also, from the symmetry of the equations one concludes that $c_r = 0$; hence the eigenvalue problem involves finding a suitable α when Re and c_i are specified. Two linearly independent solutions are obtained by setting first $A_3 = 0$ and then $A_1 = 0$. These solutions can then be superimposed with A_1 and A_3 chosen such that all but one of conditions (3.2) are satisfied; the remaining condition will be satisfied only when the proper value of α has been selected. Results for the fastest-growing wave are indicated in figure 1 as well as the stability boundary. The normalization chosen was $A_{1r} = 2$ so as to agree with the standard result $\Phi_1 = \operatorname{sech} y$ in the inviscid limit.

Finding the numerical solution of (2.8) which yields Φ_2 turns out, by contrast, to be a fairly difficult matter. The difficulty is of the same nature as that usually encountered in solving the Orr–Sommerfeld equation for bounded flows at very large values of Re, i.e. the viscous solution (multiplied by A_3 in (3.1)) grows much more rapidly than the inviscid solution. As a result, it becomes impossible to compute a linearly independent inviscid solution, because a small amount of the fast-growing viscous solution is introduced by truncation error at each step and, after several integration steps, completely dominates the results. This sort of problem seems to be particularly acute in the case of (2.8) because of its inhomogeneity and the unboundedness of the flow.

The asymptotic behaviour as $y \to -\infty$ of the general solution to (2.8) is given by

$$\Phi_2 \sim B_1 e^{2\alpha y} + B_3 \exp\left\{2\alpha\left(1+\frac{iRe}{2\alpha}\right)^{\frac{1}{2}} y\right\} + K_1 e^{2\alpha y} + K_3 \exp\left\{\alpha\left[1+\left(1+\frac{iRe}{2\alpha}\right)^{\frac{1}{2}}\right] y\right\} + K_5 \exp\left\{2\alpha\left(1+\frac{iRe}{2\alpha}\right)^{\frac{1}{2}} y\right\}, \tag{3.3}$$

which, in principle, provides the boundary conditions to be imposed at $y = -3$. Here the constants K_i denote that particular solution which would result from substituting the asymptotic form of Φ_1 into the right-hand side of (2.8). From the symmetry of Φ_1 and the knowledge that a particular solution of (2.8) will, by itself, satisfy the boundary conditions at infinity, we can also impose at $y = 0$ the conditions

$$\Phi_{2r}'(0) = \Phi_{2r}'''(0) = \Phi_{2i}(0) = \Phi_{2i}''(0) = 0. \tag{3.4}$$

Referring back now to (3.3), it can be seen that $B_1 = B_3 = 0$ and one only needs to know K_1, K_3 and K_5 to obtain the desired particular solution. However,

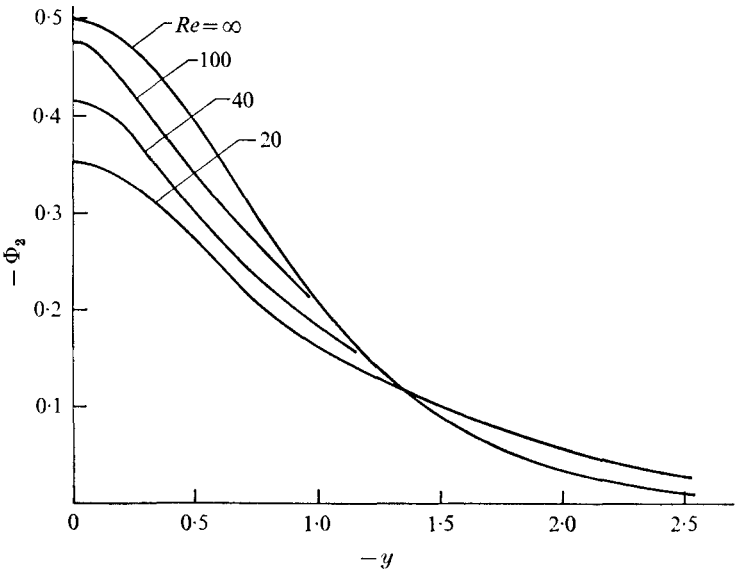

FIGURE 2. Numerical solution for Φ_2 at various values of Re compared with the analytical result $\Phi_2 = -0{\cdot}5\,\mathrm{sech}^2 y$ when $Re = \infty$.

by substituting the asymptotic form of Φ_1, as given by (3.1), into (2.8) it would be erroneously concluded that $K_1 = K_5 = 0$. To summarize these difficulties, a considerable effort would be required to obtain the exact values for the constants in the asymptotic form of the particular solution to (2.8). In particular, a more accurate representation of the behaviour of Φ_1 as $y \to -\infty$ would be required than that provided by (3.1). The equation could still be solved using an initial-value (shooting) method; however, the homogeneous solutions would have to be first included and then subtracted out using an orthonormalization technique (see, for example, Davey 1973) because the viscous solution multiplied by B_3 grows very rapidly.

A considerably simpler alternative that has been employed in the present computations is to use a finite-difference method. The latter is much easier to program than the orthonormalization technique and seems to be free of the instability that one encounters with shooting methods. Indeed Thomas (1953), who was the first to solve the Orr–Sommerfeld equation numerically (for Poiseuille flow), recognized these advantages and discussed the matter in his paper. An additional advantage in the present case is that the results in the range of interest, i.e. $|y| < 2$, were observed to be quite insensitive to the boundary conditions imposed at $y = -3$. Hence these can be set equal to zero without introducing any error of consequence.

The actual procedure employed was to rewrite (2.8) as a coupled set of four real second-order ordinary differential equations. The second derivatives were then differenced according to

$$\Phi''(y_n) \simeq (\Phi_{n+1} - 2\Phi_n + \Phi_{n-1})/h^2 + O(h^2), \tag{3.5}$$

where the step size h was taken to be 0·05. Rather than impose the boundary

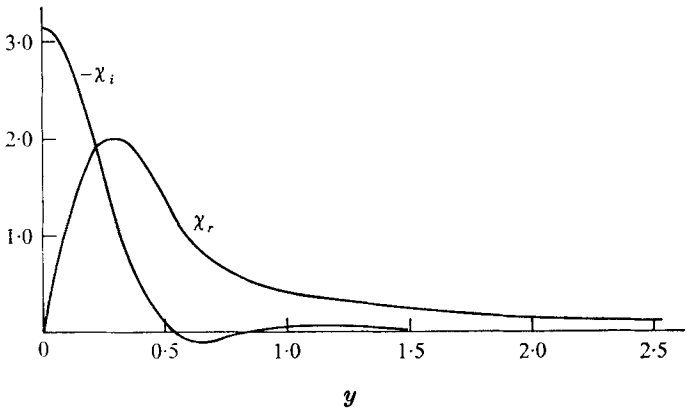

FIGURE 3. Numerical solution of the adjoint Orr–Sommerfeld equation for $Re = 150$.

conditions (3.4) in the form written, the computations were continued to $y = 0{\cdot}05$ and the even and oddness properties of Φ_2 invoked.

This procedure leads to the problem of solving a banded matrix, which was done using subroutine DGELB of the IBM SSP package. The method was found to be very fast, requiring only 9 or 10 s on an IBM 360 computer including a preliminary integration of (2.7) so that $\Phi_1(y)$ and its derivatives could be stored. Results for various values of Re are illustrated in figure 2; the solution in the inviscid limit was obtained by Schade (1964).

Proceeding now to the adjoint equation (2.10), the integration was done by the Runge–Kutta method and, following Schade, the real part of χ was chosen to be odd with the imaginary part even, so that

$$\chi_r(0) = \chi_r''(0) = \chi_i'(0) = \chi_i'''(0) = 0. \tag{3.6}$$

At $y = -3$, χ has the same behaviour as Φ_1, i.e. conditions (3.2) were used to initiate the integration. However, somewhat more care would seem to be required in solving the adjoint problem than in solving the Orr–Sommerfeld equation because in the inviscid limit $\chi_r = \operatorname{cosech} y$, which is singular at $y = 0$. Moreover, χ_i oscillates as can be seen from the solution shown in figure 3; that behaviour can be verified by noting that, for $Re \gg 1$, χ_i is given asymptotically by the Lommel function, L_r in the notation of Benney (1961), and the oscillation can be seen in figure 1 of his paper. In spite of these potential numerical difficulties, the Runge–Kutta procedure was found to be adequate as was verified by comparing some results with others obtained by the finite-difference method.

4. Results for the coefficients of the amplitude equation

Having obtained by numerical means Φ_1, χ and Φ_2, the integrals appearing in (2.11) were evaluated using Simpson's rule. Let us now define the integrals

$$\left.\begin{aligned} I_1 = -i\int_{-\infty}^{\infty} \chi(\Phi_1'' - \alpha_n^2\,\Phi_1)\,dy, \quad I_2 = \int_{-\infty}^{\infty} \chi(\bar{u}-c)\,\Phi_1\,dy \\ \text{and} \qquad I_3 = \int_{-\infty}^{\infty} \chi G\,dy. \end{aligned}\right\} \tag{4.1}$$

Re	α_n	$2\alpha_n^2 I_2/I_1$	a_2
20	0·783	−0·564	−0·552
30	0·841	−0·594	−0·786
40	0·874	−0·604	−0·951
50	0·895	−0·610	−1·105
75	0·926	−0·616	−1·35
100	0·943	−0·626	−1·504
125	0·954	−0·626	−1·61
150	0·961	−0·626	−1·685
∞	1·000	−0·636	−1·698

TABLE 1. Computed values of parameters in the amplitude evolution equation.

Because of the symmetry of their integrands, we conclude that I_1, I_2 and I_3, as defined in (4.1), are all real numbers. The non-zero portions of the integrals involve only the even part of the integrand, so that it is simply necessary to evaluate the integral from $y = -\infty$ to $y = 0$ and then double the result.

In order to relate these integrals to more familiar quantities, we rewrite (2.11) in terms of the fast time scale and also use (2.5) to obtain

$$\frac{1}{A}\frac{dA}{dt} = 2\alpha_n^2 \frac{I_2}{I_1}(\alpha - \alpha_n) - \alpha_n \epsilon^2 \frac{I_3}{I_1}|A|^2 + O(\epsilon^4). \tag{4.2}$$

The first term in (4.2) can be interpreted as the value of αc_i in the linear theory that would be obtained by expanding that quantity in a Taylor series about a point (such as A in figure 1) on the neutral-stability curve, i.e.

$$2\alpha_n^2 \frac{I_2}{I_1} = \left(\frac{\partial(\alpha c_i)}{\partial \alpha}\right)_{Re}. \tag{4.3}$$

When $Re = \infty$ the term (4.3) has the value $-2/\pi$ according to Lin's perturbation formula. Of primary interest, however, is the Landau constant, which is given by

$$a_2 = -\alpha_n I_3/I_1 \tag{4.4}$$

when we make the identification $A_1 \equiv \epsilon A$ [cf. (1.1)]. The numerical results are presented in table 1.

The value of $2\alpha_n^2 I_2/I_1$ remains fairly constant, which is in accordance with the results shown in figure 2 of Betchov & Szewczyk, i.e. the spacing between curves of constant αc_i does not change much as Re varies. The Landau constant, on the other hand, is seen to vary markedly with Re for $Re \leqslant 100$.

These results can easily be generalized to include wave trains because the extension simply involves the addition of a linear term multiplied by the group velocity $\omega'(\alpha)$. The amplitude evolution equation for nonlinear systems has the general form (see e.g. discussion by Benney & Maslowe 1975)

$$\partial A/\partial T + \omega' \partial A/\partial X = a_2 A^2 A^* + O(\epsilon^2), \tag{4.5}$$

where $X = \epsilon^2 x$ is a slow space variable, $T = \epsilon^2 t$ and ω' is a pure imaginary number for the tanh y flow. In the inviscid limit, (4.5) becomes

$$\frac{\partial A}{\partial T} - \frac{2i}{\pi}\frac{\partial A}{\partial X} = -\frac{16}{3\pi} A^2 A^*, \tag{4.6}$$

whereas for finite Re, $\omega' = 2i\alpha_n^2 I_2/I_1$ according to (4.3).

5. Concluding remarks

It was pointed out earlier that free-shear-layer experiments are usually conducted at relatively low Reynolds numbers, say $20 \leqslant Re \leqslant 100$. (Note that the Re whose values are reported by experimentalists is generally not the same as that used in stability calculations owing to differences in scaling conventions; the conversion can be accomplished roughly, according to the data of Freymuth (1966), if the experimental Re is divided by 4.) In most experiments, it is observed that initially the fastest-growing mode has the wavenumber and growth rate predicted by linearized theory. This wave then equilibrates at some finite amplitude; further downstream, subharmonic modes are destabilized, the most prominent of which has a frequency half that of the fundamental. The corresponding theory for this subharmonic resonance has been given by Kelly (1967). Eventually, three-dimensional effects become important and transition to turbulence occurs shortly thereafter.

Ideally, a weakly nonlinear approach such as the present one could be used to describe the initial exponential growth and subsequent equilibration of the linearly most unstable wave. The resultant equilibrated state could then be used as input for a theory such as that due to Kelly describing the evolution of the subharmonics. (Not having such a periodic solution, Kelly instead used the linear eigenfunction for an unstable wave after observing that this corresponded reasonably well with some of the experimental data.)

There are a number of reasons, however, why the present results ought not to be compared directly with experiment. First of all, in the experiments unstable modes grow in space rather than time, and second, the parallel-flow assumption becomes less accurate at lower Reynolds numbers. Most important, however, is the already mentioned fact that the fastest-growing wave of linear theory has an α that is too far from its neutral value for the amplitude equation to apply for very long; certainly the expansion becomes invalid long before equilibrium is reached. On the other hand, the Landau equation should describe well the initial departure from exponential growth and, owing to the reduction of a_2 at finite Re, (4.2) should apply for a longer period of time than one would have anticipated from the inviscid result.

The reduction of $|a_2|$ *vis-à-vis* the limit of infinite Re considered by Schade will be somewhat less than the figures in table 1 indicate because of the neglect of mean-flow distortion. As shown by Stuart [1960, equation (6.3)], this term will always make a negative contribution to a_2. However, there is reason to believe that the distortion is less pronounced for free shear layers than for most other flows. Essentially, the velocity distortion is produced by the Reynolds

stresses, which are zero for a neutral mode at infinite Re (this is not usually true, for example, in the case of a wake). Whatever Reynolds stress is produced at finite Re goes partly into distortion but primarily into increasing the rate of growth of the shear layer. Strong evidence that the distortion of a growing shear layer is not large during the early stages of transition is provided by the mean-flow measurements of Browand (1966, figure 5). These measurements show that, when the velocity profile is suitably non-dimensionalized, the distortion is particularly small near $y = 0$, which is where most of the contribution to a_2 would take place.

During the present investigation, some computations were also made for the mean velocity profile $\bar{u}(y) = \text{erf}\,(\frac{1}{2}\pi^{\frac{1}{2}}y)$. Although the linear eigensolution for this case is nearly identical to that of the $\tanh y$ profile, the function Φ_2 has a smaller amplitude and the Landau constant is reduced accordingly. The reduction in absolute value was of the order of 50%. This sensitivity of the weakly nonlinear theory to the details of the velocity profile was quite unexpected.

Finally, it should be mentioned that an extension of this work to stably stratified mixing layers could prove to be highly worthwhile because the amplification rates are smaller in that case. The results of a weakly nonlinear theory ought to be relevant throughout the important Richardson number range 0·15–0·35. Some of the author's as yet unpublished calculations show in fact that subcritical instability can occur for a shear layer with a $\tanh y$ velocity profile and the density profile $\bar{\rho} = \exp(-\beta \tanh y)$. Moreover, it appears from the numerical computations of Patnaik, Sherman & Corcos (1976), who integrated the nonlinear Boussinesq equations, that subharmonic resonance occurs just as it does in the homogeneous case. Experiments with stratified shear flows have also been reported by, among others, Scotti & Corcos (1972) and Browand & Winant (1973); however, comparisons of their data with theory might prove to be difficult because of the spatial variations in mean-flow properties that occurred during the experiments.

The author is pleased to acknowledge some very helpful suggestions of Prof. Alan Needleman and Prof. Steven Orszag of M.I.T. concerning the numerical aspects of this work and the programming assistance of Mr Richard Dubois of McGill University. This research was supported by the U.S. National Oceanic and Atmospheric Administration and the National Research Council of Canada.

Appendix. An estimate of the distortion effect

An interesting feature exhibited by the weakly nonlinear theory is that the Reynolds stress due to the self-interaction of the fundamental disturbance mode causes an $O(\epsilon^2)$ distortion of the mean velocity profile. The magnitude of the Landau constant is altered as a result. For a parallel shear flow, the mean velocity has the form (Stuart 1960)

$$u(y, \tau) = \bar{u}(y) + \epsilon^2 A A^* f(y), \tag{A 1}$$

where $\bar{u} = \tanh y$ in the present case. The quantity f satisfies the ordinary differential equation

$$f'' = i\alpha_n Re(\Phi_1'' \Phi_1^* - \Phi_1''^* \Phi_1), \tag{A 2}$$

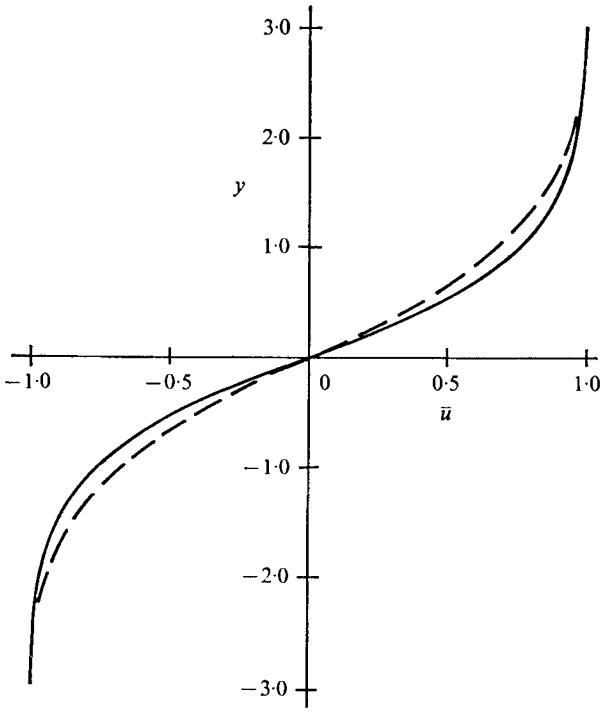

FIGURE 4. Laminar mean flow and anticipated mean flow with distortion. ——, $\bar{u} = \tanh y$; – – –, distorted flow.

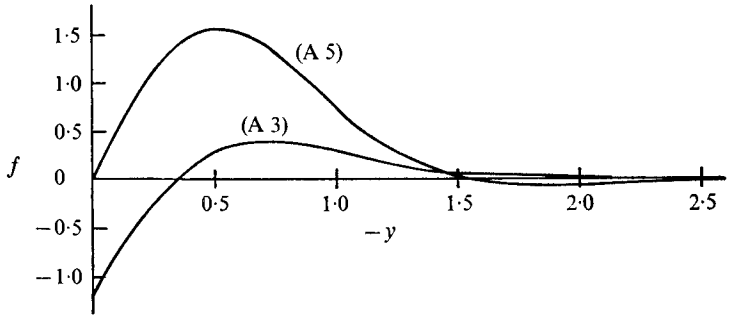

FIGURE 5. Numerical solution of distortion equations for steady and temporally growing mean parallel flow; $Re = 40$.

whose solution is given by

$$f(y) = i\alpha_n Re \int_{-\infty}^{y} (\Phi_1' \Phi_1^* - \Phi_1'^* \Phi_1)\, dy. \tag{A 3}$$

With $f \neq 0$, the function $G(y)$ defined below (2.9) contains the following additional terms:

$$f(\Phi_1'' - \alpha_n^2 \Phi_1) - f'' \Phi_1. \tag{A 4}$$

For a steady parallel shear flow one would expect from energy considerations that the flow would distort as indicated in figure 4 and, indeed, it can be deduced from (A 3) that $f(y)$ is an odd function for the $\tanh y$ shear layer. However,

numerical integration of this equation leads to the result shown in figure 5. Although this result seems qualitatively correct for $|y| \geqslant 0{\cdot}5$, f does not return to zero at $y = 0$ but has a nearly singular behaviour. An equally serious difficulty is that the integral in (A 3) behaves, according to the numerical results, as $Re^{-0{\cdot}9}$ for large Re; hence f becomes unbounded instead of approaching zero as $Re \to \infty$.

These difficulties are related to the fact that the basic flow is not a solution of the Navier–Stokes equations at finite Reynolds number. The proper resolution would be to consider a growing shear layer; in that case, the governing partial differential equations are no longer separable. A much less ambitious approach is described here whose objective is at least to obtain some estimate of the magnitude of the terms appearing in (A 4) and of their contribution to a_2. To that end we first consider a shear layer growing slowly in time such that

$$y = y^*/L(t),$$

where y^* is dimensional, L is the length scale (now slowly growing) and $\bar{u}$ depends upon y, as before. The mean-flow equation becomes

$$f'' + \tfrac{1}{2}LL'yf' = i\alpha_n Re\,(\Phi_1'' \Phi_1^* - \Phi_1''^* \Phi_1). \tag{A 5}$$

Equation (A 5) is an improvement over (A 2) because it admits solutions with $f(0) = 0$. One such solution is shown in figure 5, corresponding to $\bar{u} = \operatorname{erf}(\frac{1}{2}\pi^{\frac{1}{2}}y)$, in which case $LL' = \frac{1}{2}\pi\nu$. However, the difficulty at large Re remains; also, in this approach α_n and Re vary with time, so that the 'Landau constant' is no longer constant.

A parallel and, as it turns out, more interesting approach is to consider a shear layer growing in space. We note, first of all, that when the velocity difference $2U$ across the mixing layer is smaller than the mean velocity U_0 an approximate solution of the boundary-layer equations is

$$\bar{u}^* - U_0 = U \operatorname{erf}(\pi^{\frac{1}{2}}y^*/2L), \tag{A 6}$$

where $L(x) = (\pi\nu x/U_0)^{\frac{1}{2}}$. From the continuity equation, the dimensionless vertical component of velocity is found to be

$$v = (-2/\pi)\,L' \exp(-\tfrac{1}{4}\pi y^2). \tag{A 7}$$

The constant of integration has been chosen such that $v(\infty) = v(-\infty) = 0$. Note that the dividing streamline now has a negative slope, which agrees with the results of Ting (1959), and that his boundary condition $u(\infty)v(\infty) = u(-\infty)v(-\infty)$ is satisfied by (A 7).

With a non-zero vertical component of the mean velocity, the equation for f now becomes

$$f'' + (U/U_0)\exp(-\tfrac{1}{4}\pi y^2)f' = \alpha_n Re\,(\Phi_1'' \Phi_1^* - \Phi_1''^* \Phi_1) \tag{A 8}$$

with boundary conditions $f(\infty) = f(-\infty) = 0$; significantly, f is no longer an odd function, which may partly explain the very asymmetric mean-flow distortion observed in Browand's experiments. Also, Φ_1 now satisfies the so-called 'modified Orr–Sommerfeld equation', i.e. (2.7) contains the following additional term:

$$i(\alpha_n Re)^{-1}(U/U_0)\exp(-\tfrac{1}{4}\pi y^2)\,(\Phi_1''' - \alpha_n^2 \Phi_1'). \tag{A 9}$$

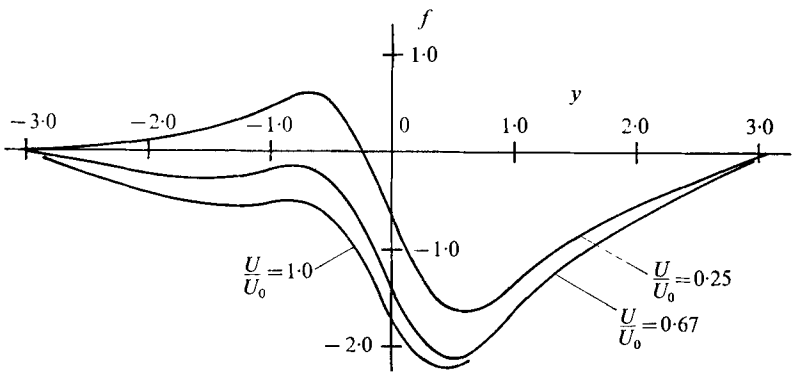

FIGURE 6. Distortion quantity for spatially growing shear layer; $Re = 40$.

Solutions of (A 8) have been obtained for various combinations of Re and U/U_0. A strong dependence upon the latter parameter was observed as is shown by the results plotted in figure 6. The value $U/U_0 = 0{\cdot}67$ corresponds to the experiments of Miksad, whereas in Browand's experiments $U/U_0 = 1$. The distortion shown is very similar to the experimental data except that the maximum distortion in the experiments occurred at larger values of $|y|$. This discrepancy is more than likely due to the incomplete consideration of the effects of non-parallel flow in the calculations.

As for the Landau constant itself, it is difficult to estimate the distortion effect because the use of the modified Orr–Sommerfeld equation did not completely resolve the tendency of f to increase with Re. Under the circumstances, it seems reasonable to impose the proper behaviour artificially by evaluating the Reynolds stress quantity in parentheses in (A 8) at some higher value of Re. It was found that using $Re^{\frac{3}{2}}$ led to a plausible rate of decay at large Re, thus facilitating comparison with the results of Schade (1964) and Stuart (1967), who imposed the condition of zero velocity distortion.

It should be noted that this procedure requires the solution of the modified Orr–Sommerfeld equation at very high values of Re. A program using the finite-difference method was written for that purpose and no difficulties were experienced even for Re as large as 5000. At a nominal value of $Re = 40$ with $U/U_0 = 0{\cdot}66$, it was found that $a_2 = -1{\cdot}35$ as compared with the value $-0{\cdot}951$ without distortion. This result suggests that the effect of distortion may not be negligible, although one can not say so definitely until a full analysis has been conducted for a growing shear layer.

In summary, the present calculations show that, in order to make a serious quantitative comparison of the weakly nonlinear theory with shear-layer experiments at finite Re, it would be necessary to employ the true experimental velocity profile, and to take account of both spatial variations and distortion, the Landau constant being sensitive to all of these effects.

The author is indebted to Professor R. E. Kelly for some most helpful discussions concerning the material presented in this appendix.

REFERENCES

BENNEY, D. J. 1961 *J. Fluid Mech.* **10**, 209.

BENNEY, D. J. & MASLOWE, S. A. 1975 *Stud. Appl. Math.* **54**, 181.

BETCHOV, R. & SZEWCZYK, A. 1963 *Phys. Fluids*, **6**, 1391.

BROWAND, F. 1966 *J. Fluid Mech.* **26**, 281.

BROWAND, F. & WINANT, C. 1973 *Boundary-Layer Met.* **5**, 67.

DAVEY, A. 1973 *Quart. J. Mech. Appl. Math.* **26**, 401.

FREYMUTH, P. 1966 *J. Fluid Mech.* **25**, 683.

KELLY, R. E. 1967 *J. Fluid Mech.* **27**, 657.

MICHALKE, A. 1964 *J. Fluid Mech.* **19**, 543.

MIKSAD, R. W. 1972 *J. Fluid Mech.* **56**, 695.

PATNAIK, P., SHERMAN, F. & CORCOS, G. 1976 *J. Fluid Mech.* **73**, 215.

SCHADE, H. 1964 *Phys. Fluids*, **7**, 623.

SCOTTI, R. S. & CORCOS, G. M. 1972 *J. Fluid Mech.* **52**, 499.

SHANKS, D. 1955 *J. Math. & Phys.* **34**, 1.

STUART, J. T. 1960 *J. Fluid Mech.* **9**, 353.

STUART, J. T. 1967 *J. Fluid Mech.* **29**, 417.

THOMAS, J. H. 1953 *Phys. Rev.* **91**, 780.

TING, L. 1959 *J. Math. & Phys.* **38**, 153.

WATSON, J. 1960 *J. Fluid Mech.* **9**, 371.